

# Study of the magnetic state of $\text{K}_{0.8}\text{Fe}_{1.6}\text{Se}_2$ using the five-orbital Hubbard model in the Hartree-Fock approximation

Qinlong Luo,<sup>1,2</sup> Andrew Nicholson,<sup>1,2</sup> José Riera,<sup>3</sup> Dao-Xin Yao,<sup>4</sup> Adriana Moreo,<sup>1,2</sup> and Elbio Dagotto<sup>1,2</sup>

<sup>1</sup>Department of Physics and Astronomy, The University of Tennessee, Knoxville, TN 37996

<sup>2</sup>Materials Science and Technology Division, Oak Ridge National Laboratory, Oak Ridge, TN 32831

<sup>3</sup>Instituto de Física Rosario, Universidad Nacional de Rosario, 2000-Rosario, Argentina

<sup>4</sup>State Key Laboratory of Optoelectronic Materials and Technologies,

Sun Yat-sen University, Guangzhou 510275, China

(Dated: September 9, 2011)

Motivated by the recent discovery of Fe-based superconductors close to an antiferromagnetic insulator in the experimental phase diagram, here the five-orbital Hubbard model (without lattice distortions) is studied using the real-space Hartree-Fock approximation, employing a  $10 \times 10$  Fe cluster with Fe vacancies in a  $\sqrt{5} \times \sqrt{5}$  pattern. Varying the Hubbard and Hund couplings, and at electronic density  $n=6.0$ , the phase diagram contains an insulating state with the same spin pattern as observed experimentally, involving  $2 \times 2$  ferromagnetic plaquettes coupled with one another antiferromagnetically. The presence of local FM tendencies is in qualitative agreement with Lanczos results for the three-orbital model also reported here. The magnetic moment  $\sim 3\mu_B/\text{Fe}$  is in good agreement with experiments. Several other phases are also stabilized in the phase diagram, in agreement with recent calculations using phenomenological models.

*Introduction.* Among the most recent exciting developments in the field of Fe-based superconductors<sup>1</sup> is the discovery of superconductivity (SC) with  $T_c \sim 30$  K in the heavily electron-doped 122 iron-chalcogenides  $\text{K}_{0.8}\text{Fe}_{2-x}\text{Se}_2$  and  $(\text{Ti},\text{K})\text{Fe}_{2-x}\text{Se}_2$  compounds.<sup>2</sup> These materials contain ordered Fe vacancies in the FeSe layers, increasing the complexity of these systems. Recent neutron scattering results for the parent compound  $\text{K}_{0.8}\text{Fe}_{1.6}\text{Se}_2$ ,<sup>3</sup> with the Fe-vacancies arranged in a  $\sqrt{5} \times \sqrt{5}$  pattern, revealed an unexpected magnetic and insulating state involving  $2 \times 2$  Fe plaquettes that have their four Fe spins ferromagnetically ordered, and with these plaquettes coupled to each other antiferromagnetically.<sup>4</sup> The ordered magnetic moment is  $3.31 \mu_B/\text{Fe}$ , the largest among all Fe pnictide and chalcogenide superconductors, and the magnetic transition occurs at a high temperature  $T_N \approx 559$  K. Angle-resolved photoemission experiments for  $(\text{Ti}, \text{K})\text{Fe}_{1.78}\text{Se}_2$  have revealed a Fermi surface (FS) with only electron-like pockets at the  $(\pi, 0)$  and  $(0, \pi)$  points and a nodeless superconducting gap at those pockets.<sup>5</sup> The superconducting phase in these compounds cannot be explained by the nesting between hole and electron pockets.<sup>5,6</sup> Moreover, the resistivity of these materials displays a behavior corresponding to an insulator in a robust range of the Fe concentration  $x$ ,<sup>7</sup> suggesting that SC may arise from the doping of a Mott insulator, as in the cuprates. All these results certainly have challenged prevailing ideas for the origin of SC in these materials that were originally based on a nested FS picture and a metallic parent state.

Several theoretical efforts have recently addressed the exotic magnetic state that appears in the presence of vacancies. Band structure calculations described this state as an antiferromagnetic insulator with a gap  $\sim 0.4$ - $0.6$  eV.<sup>8,9</sup> Several model Hamiltonian calculations have also been presented and, in particular, two recent publications are important to compare our results against.

Yu *et al.*<sup>10</sup> analyzed this problem using a phenomenological  $J_1$ - $J_2$  spin model (see also Ref. 8) with nearest-neighbors (NN) and next-NN terms superexchange couplings, studied via classical Monte Carlo. In this analysis the couplings inside the  $2 \times 2$  plaquettes and those between plaquettes were allowed to be different, and also to take positive or negative values. Five antiferromagnetic phases, including the phase found experimentally<sup>3</sup> in  $\text{K}_{0.8}\text{Fe}_{1.6}\text{Se}_2$ , which was dubbed “AF1”, were found varying the  $J_1$  and  $J_2$  couplings.<sup>11</sup> From a different perspective that relies on a two-orbital ( $d_{xz}$  and  $d_{yz}$ ) spin-fermion model for pnictides, and with tetramer lattice distortion incorporated, Yin *et al.*<sup>12</sup> studied the regime of electronic density  $n=1$  (one electron per Fe), where they also reported the presence of an AF1 state, found competing with a “C” type state with wavevector  $(\pi, 0)$ .

In the present publication, a more fundamental five-orbital Hubbard model, without lattice distortions, is investigated. Our main result is that increasing the Hubbard coupling  $U$  and the Hund coupling  $J$ , a robust region of stability of the AF1 state is found. Our effort allows to display the regions of dominance of the many competing states in terms of  $U$  and  $J/U$ , facilitating a discussion on possible phase transitions among these states by varying experimental parameters. A sketch of the AF1 state and its two main competitors, the C and AF4 states, is in Fig. 1. Our results agree qualitatively in several respects with the phenomenological studies of Refs. 10,12 particularly if a combination of results of these investigations is made. Finally, also note that a recent study<sup>13</sup> of the three-orbital Hubbard model<sup>14</sup> using mean-field techniques<sup>15</sup> has also reported the existence of an AF1 state but with orbital order (OO). The relation with our results will also be discussed below.

*Models and methods.* In this manuscript, the standard multiorbital Hubbard model will be used. This model has been extensively described in several previous pub-

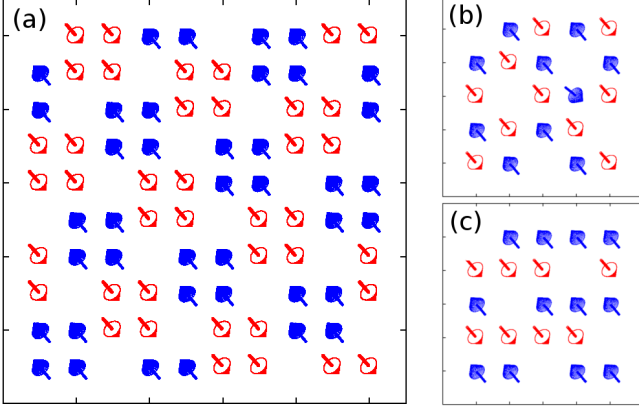


FIG. 1: (Color online) (a) Sketch of the AF1 state found to be stable in a region of the  $U$ - $J/U$  phase diagram (see Fig. 2) in our HF approximation to the five-orbital Hubbard model, in agreement with neutron diffraction.<sup>3</sup> (b) A competing state dubbed AF4 (stable at smaller  $J/U$ 's in Fig. 2). (c) The C competing state. For (b) and (c), a subset of the  $10 \times 10$  cluster used is shown.

lications, by our group and others. More specifically, the model used is the five-orbital Hubbard model defined explicitly in Ref. 15 with the hopping amplitudes introduced by Graser *et al.*<sup>16</sup> By construction, this model has a FS that is in close agreement with band structure calculations and angle-resolved photoemission results for the pnictides without vacancies. The presence of the realistic AF1 state in our results, as shown below, suggests that the same set of hopping amplitudes can be used in a system with Fe vacancies. The electronic density will be  $n=6.0$ , i.e. 6 electrons per Fe, for all the five-orbital model results presented below. The couplings are the on-site Hubbard repulsion  $U$  at the same orbital and the on-site Hund coupling  $J$ . The on-site inter-orbital repulsion  $U'$  satisfies  $U'=U-2J$ . The computational method that is employed to extract information from this five-orbital model relies on the study of a  $10 \times 10$  cluster, as sketched in Fig. 1(a), using periodic boundary conditions. In this cluster, several vacancies and  $2 \times 2$  building blocks fit comfortably inside, giving us confidence that the main local tendencies to magnetic order are not dramatically affected by size effects.

With regards to the actual many-body technique used to study the  $10 \times 10$  cluster, here the real-space Hartree-Fock (HF) approximation was employed. The method is a straightforward generalization of that used recently by our group in Ref. 17 in the study of charge stripe tendencies for the two-orbital model. This HF real-space approach was preferred over a momentum-space procedure in order to allow for the system to select spontaneously the state that minimizes the HF energy, at least for the finite cluster here employed. In practice, the many fermionic expectation values that appear in the HF formalism must be found iteratively by energy

minimization. At the beginning of the iterative process, both random initial conditions as well as initial ordered states favoring the many phases that are anticipated to be in competition were employed. After each of the computer runs using different initial conditions have reached convergence, at a fixed  $U$  and  $J/U$ , a mere comparison of energies allowed us to find the ground state for those particular couplings. In our setup, typical running times for one set of couplings  $U$ - $J/U$  required approximately 20 hours of CPU time to reach convergence.<sup>18</sup> Dozens of computer cluster nodes have been used to complete our analysis in a parallel manner.

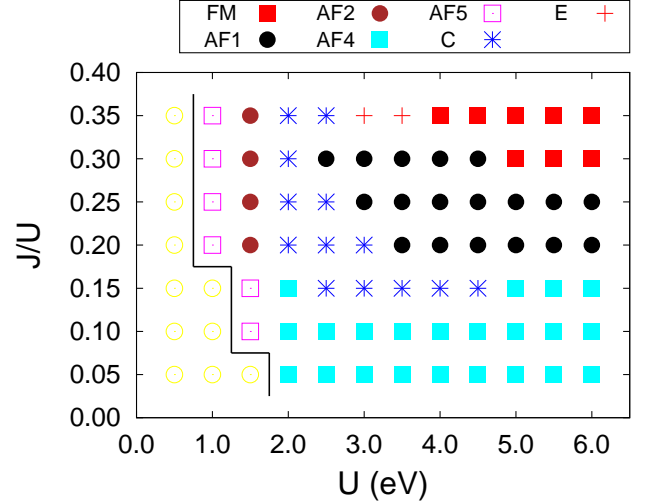


FIG. 2: (Color online) Phase diagram of the five-orbital Hubbard model with  $\sqrt{5} \times \sqrt{5}$  Fe vacancies studied via the real-space HF approximation to a  $10 \times 10$  cluster, employing the procedure for convergence described in the text. With increasing  $U$ , clear tendencies toward magnetic states are developed. The realistic AF1 state found in neutron scattering experiments<sup>3</sup> appears here above  $J/U=0.15$  and for  $U$  larger than 2.5 eV. The notation for the most important states is explained in Fig. 1 and for the rest in Refs. 8,10,12. The region with low-intensity yellow circles at small  $U$  is non-magnetic.<sup>19</sup>

**Results.** The main results arising from the computational minimization process just described are summarized in the phase diagram shown in Fig. 2. Since the hopping parameters of Ref. 16 are already in eV units, our Hubbard coupling  $U$  is also displayed in the same units. The notation for the many competing phases used here is that of Refs. 8,10,12 to facilitate comparisons. The main result of the present work is that our phase diagram displays a robust region where the magnetic order unveiled by neutron diffraction,<sup>3</sup> see Fig. 1(a), is found to be stable. The ratio  $J/U$  needed for the AF1 phase to be the ground state is in good agreement with previous estimations for the same model, although obtained in the absence of vacancies, based on the comparison of Hubbard model results against neutron and photoemission data.<sup>15</sup> The ratio  $J/U$  is surprisingly similar between the pnictides and the chalcogenides. With regards to the

actual value of  $U$  in eV's, the range unveiled in previous investigations that focused on the "1111" and "122" families of pnictides was approximately 1.5 eV (see Fig. 13 of Ref. 15). The increase to 2.5 eV in the present investigation is not surprising in view of the more insulating characteristics of materials such as  $\text{K}_{0.8}\text{Fe}_{1.6}\text{Se}_2$ , and suggests that merely adding vacancies to the intermediate  $U$  state of the pnictides (without vacancies) is not sufficient to stabilize the AF1 state but an increase in  $U$  is also needed. Finally, with regards to OO, none is observed in the AF1 state in the range of  $U$  shown in Fig. 2, i.e. for  $U \leq 6$  eV. In this range, the electronic density of all the orbitals ( $d_{xz}$  and  $d_{yz}$  in particular) is independent of the site location in the cluster analyzed. However, upon further increasing  $U$  to 8 eV and beyond, the *same* OO pattern found in the three-orbital model<sup>13</sup> appears in our calculations (not shown explicitly), with the populations of the  $d_{xz}$  and  $d_{yz}$  orbitals now being different at all sites. It seems that with five orbitals the AF1 state manifests itself both with and without OO, depending on  $U$ , while for three orbitals the intermediate phase with AF1 magnetic order and without OO is not present.<sup>13</sup>

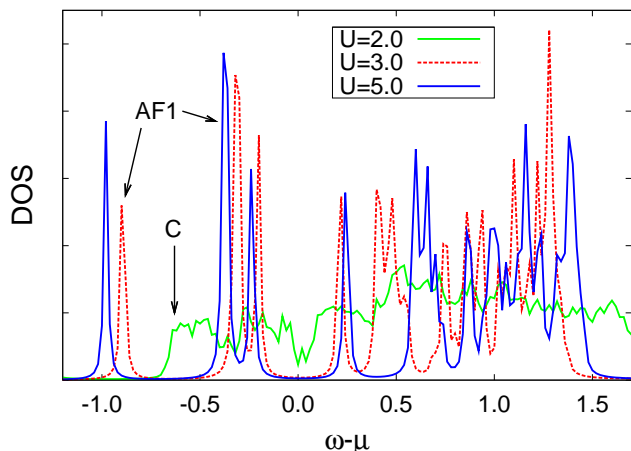


FIG. 3: (Color online) Density of states of the AF1 and C phases sketched in Figs. 1(a,c), at the  $U$ 's indicated,  $J/U=0.25$ , and using a  $10 \times 10$  cluster. The gap at the chemical potential suggests that the AF1 state ( $U=3$  and 5) is an insulator, although with a mild  $U$  dependence in the value of this gap. On the other hand, the C state appears to have only a pseudogap at the Fermi level.<sup>20</sup>

Together with the realistic AF1 phase, Fig. 2 reveals several other states, and two of them are prominent. Keeping the ratio  $J/U$  constant but reducing  $U$ , the previously described C-type state (Fig. 1(c)) was found to be stable. This is reasonable since without Fe vacancies this state is the dominant spin order in the intermediate range of couplings, where the ground state is both metallic and magnetic.<sup>15</sup> In  $\text{K}_{0.8}\text{Fe}_{1.6}\text{Se}_2$ , as the bandwidth is increased by, e.g., increasing the pressure, a transition from the AF1 to the C-state could be experimentally observed. In these regards, our conclusions agree with Ref. 12 that the C-state is the main competitor of the

AF1 state. However, note that other states reported in Ref. 10 are also present in our phase diagram. For instance, the AF4 state (Fig. 2(b)) is stable in a large region of parameter space at small values of  $J/U$ . Thus, overall our results support a combination of the main conclusions of Refs. 10,12.

The density-of-state (DOS) for the AF1 phase is shown in Fig. 3 for representative couplings. The presence of a gap at the chemical potential indicates an insulating state, in agreement with experiments.<sup>3</sup> This is not surprising considering that the transport of charge from each  $2 \times 2$  building block to a NN block may be suppressed due to the effective antiferromagnetic coupling between blocks, at least at large  $U$  and  $J$ . In other words, using a tilted square lattice made out of  $2 \times 2$  superspin blocks, the state is actually a staggered antiferromagnet that is known to have low conductance. On the other hand, it is interesting to observe that the AF1 gap is only weakly dependent on  $U$ , suggesting that not only the increase in  $U$  is responsible for the insulating behavior but there must be other geometrical reasons that may contribute to the gap through quantum interference. This is reminiscent of results reported years ago for the insulating CE phase of half-doped manganites, state that is stabilized in the phase diagram even in the absence of electron-phonon coupling due to the peculiar geometry of the zigzag chains involved in the CE state and the multi-orbital nature of the problem, that induces a band insulating behavior.<sup>21</sup> Thus, in agreement with recent independent observations,<sup>12</sup> our results suggest that the insulator stabilized in the presence of Fe vacancies may have a dual Mott and band-insulating character. Note also that the competing C-state only has a pseudogap (Fig. 3), and thus it may be a bad metal.<sup>20</sup>

With regards to the strength of the FM tendencies in each of the  $2 \times 2$  building blocks of the AF1 state, examples of the values of the magnetic moment  $m$  (in Bohr magnetons, assuming  $g=2$ , and at  $J/U=0.25$ ) are  $m=3.87$  ( $U=3.0$ ),  $m=3.93$  ( $U=4.0$ ), and  $m=3.95$  ( $U=5.0$ ), in good agreement with neutron diffraction results<sup>3</sup>  $m=3.3$ . Thus, the Fe spins in the AF1 superblocks are near the saturation value  $4.0 \mu_B$  at  $n=6.0$ . Note that the competing C-phase also has a surprisingly large moment  $m=3.5$  at  $U=2.0$  and  $J/U=0.25$ .

*Results for the three-orbital Hubbard model.* The results reported thus far have been obtained under the HF approximation. Better unbiased approximations for this model are not currently available. However, at least consistency checks of the present results can be carried out using the Lanczos technique restricted to the  $2 \times 2$  cluster of irons that forms the AF1 state. For our problem, an additional simplification from five to three orbitals ( $d_{xz}$ ,  $d_{yz}$ , and  $d_{xy}$ ) is needed to reduce the Hilbert space to a reasonable size, thus here the model introduced by Daghofer *et al.*<sup>14</sup> was used. The present Lanczos study is equivalent to a 12-sites one-orbital Hubbard model which can be done comfortably with present day computers even with the open boundary conditions (OBC)

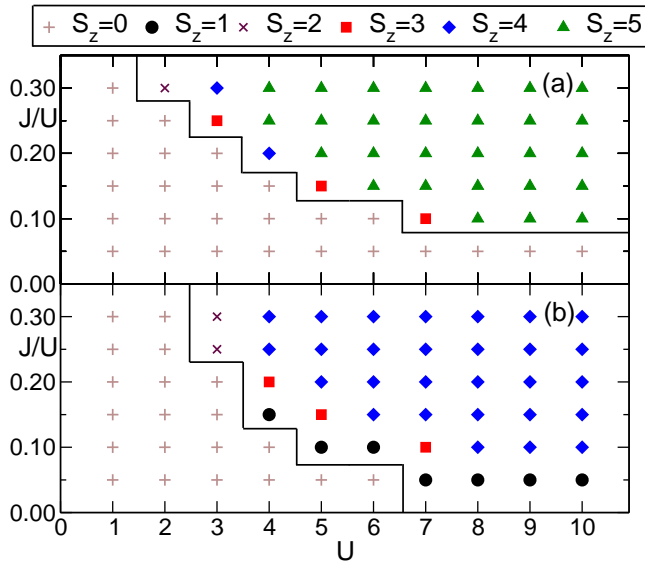


FIG. 4: (Color online) Total spin of a  $2 \times 2$  cluster using the three-orbital Hubbard model<sup>14</sup> and the Lanczos technique, varying  $U$  and  $J/U$ . Panel (a) is for 10 electrons, while (b) is for 14 electrons. The “undoped” limit is for 16 electrons in the three-orbital model.<sup>14</sup> The figure shows that in these hole doped clusters FM tendencies develop as  $U$  grows, at realistic  $J/U$ ’s, compatible with the five-orbital HF results.

employed here.<sup>22</sup> Our focus has been on the total spin quantum number to search for indications of FM tendencies in the  $2 \times 2$  cluster. The main results are in Fig. 4 for the case of hole doping. These results indicate that with increasing  $U$  and  $J/U$ , FM tendencies indeed develop, in agreement with the five-orbital HF results (Fig. 2). With electron doping also FM tendencies were found (not shown). In these Lanczos results the transition from low- to high-spin is rather abrupt. However, note that in the  $2 \times 2$  cluster there is obviously no room to distinguish a

fully FM state from an AF1 state, thus the large-spin region of the  $2 \times 2$  cluster may correspond to any of the two if larger clusters could be studied. Nevertheless, solving exactly this case allows us to confirm that with increasing  $U$  (at realistic  $J/U$ ’s), there is a clear tendency in the multiorbital Hubbard model towards local FM order in  $2 \times 2$  clusters.

*Summary.* Real-space HF-approximation results for the five-orbital Hubbard model, supplemented by Lanczos calculations for three-orbital on a  $2 \times 2$  plaquette, have been presented for the case of a  $\sqrt{5} \times \sqrt{5}$  arrangement of Fe vacancies. The phase diagram obtained by varying  $U$  and  $J/U$  contains the magnetic state found in neutron diffraction experiments.<sup>3</sup> This state arises at intermediate couplings  $U$  and  $J/U$ , and in the phase diagram it is not in contact with the paramagnetic metallic state of the weak coupling limit. Thus, FS nesting cannot explain the stability of the AF1 magnetic state in the presence of Fe vacancies.<sup>12</sup> The density of states shows that the AF1 state is an insulator, but since the gap does not present a strong dependence on  $U$  its origin may reside in a combination of Hubbard and band-insulator features. In agreement with recent spin<sup>10</sup> and spin-fermion<sup>12</sup> model calculations, several other magnetic phases were found here, suggesting that transitions among these competing states, or among AF1 with and without OO,<sup>13</sup> could be observed experimentally particularly by modifications in the carrier’s bandwidth.

*Acknowledgments.* Work supported by the U.S. Department of Energy, Office of Basic Energy Sciences, Materials Sciences and Engineering Division (Q.L., A.N., A.M., E.D.), CONICET, Argentina (J.R.), and the NSFC-11074310 and Fundamental Research Funds for the Central Universities (D.X.Y.). The computational studies used the Kraken supercomputer of the National Institute for Computational Sciences.

- <sup>1</sup> For a recent review, see D. C. Johnston, Adv. Phys. **59**, 803 (2010), and references therein.
- <sup>2</sup> J. Guo *et al.*, Phys. Rev. B **82**, 180520(R) (2010); M. Fang *et al.*, EPL **94**, 27009 (2011).
- <sup>3</sup> W. Bao *et al.*, Chinese Phys. Lett. **28**, 086104 (2011).
- <sup>4</sup> This magnetic state may coexist with a non-magnetic one in a nanoscale phase separated arrangement (see A. Ricci *et al.*, Phys. Rev. B **84**, 060511(R) (2011)).
- <sup>5</sup> X.-P. Wang *et al.*, EPL **93**, 57001 (2011).
- <sup>6</sup> K. Wang, H. Lei, and C. Petrovic, Phys. Rev. B **83**, 174503 (2011), and references therein.
- <sup>7</sup> M. H. Fang *et al.*, EPL **94**, 27009 (2011).
- <sup>8</sup> Chao Cao and Jianhui Dai, Phys. Rev. Lett. **107**, 056401 (2011); Phys. Rev. B **83**, 193104 (2011).
- <sup>9</sup> Xun-Wang Yan *et al.*, Phys. Rev. B **83**, 233205 (2011).
- <sup>10</sup> R. Yu, P. Goswami, and Q. Si, arXiv:1104.1445.
- <sup>11</sup> A related study also using a spin model can be found in Chen Fang *et al.*, arXiv:1103.4599.
- <sup>12</sup> Wei-Guo Yin, Chia-Hui Lin, and Wei Ku, arXiv:1106.0881

- <sup>13</sup> W. Lv, W.C. Lee, and P. W. Phillips, arXiv:1105.0432.
- <sup>14</sup> Maria Daghofer *et al.*, Phys. Rev. B **81**, 014511 (2010).
- <sup>15</sup> Qinlong Luo *et al.*, Phys. Rev. B **82**, 104508 (2010).
- <sup>16</sup> S. Graser *et al.*, New J. Phys. **11**, 025016 (2009).
- <sup>17</sup> Qinlong Luo *et al.*, Phys. Rev. B **83**, 174513 (2011).
- <sup>18</sup> The method used is described in D. D. Johnson, Phys. Rev. B **38**, 12807 (1988), with linear mixing parameter  $\alpha=0.5$ .
- <sup>19</sup> However, a very small FM moment  $m \sim 0.02$  systematically appeared in our numerical study in portions of the “non-magnetic” small  $U$  region. This subtle effect will be investigated in future efforts since it is unrelated to the large moments found in  $\text{K}_{0.8}\text{Fe}_{1.6}\text{Se}_2$ .
- <sup>20</sup> The competing AF4 state was found to be an insulator (not shown) with a large gap  $\sim 1.4$  eV.
- <sup>21</sup> T. Hotta *et al.*, Phys. Rev. Lett. **84**, 2477 (2000).
- <sup>22</sup> For technical details of the Lanczos technique see A. Nicholson *et al.*, Phys. Rev. Lett. **106**, 217002 (2011); and A. Moreo *et al.*, Phys. Rev. B **79**, 134502 (2009).